Enhancement of ionic current and charge movement by coexpression of calcium channel β_{1A} subunit with α_{1C} subunit in a human embryonic kidney cell line

Timothy J. Kamp, M. Teresa Pérez-García and Eduardo Marban*

Section of Molecular and Cellular Cardiology, Department of Medicine, Johns Hopkins University, Baltimore, MD 21205, USA

1. Coexpression of the β subunit with the α_{1C} subunit of the cardiac L-type Ca^{2+} channel has been shown to increase ionic current. To examine the mechanism of this increase, ionic and gating currents were measured in transiently transfected HEK293 cells.

2. β_{1A} subunit coexpression increased the maximal whole-cell conductance (G_{max}) measured in 10 mM Ba^{2+} from 91 ± 11 to 833 ± 107 pS pF^{-1} without a change in the voltage dependence of activation ($V_{½}$: $-6{\cdot}1 \pm 1{\cdot}1$ and $-6{\cdot}6 \pm 0{\cdot}9$ mV, respectively).

3. Gating currents were smaller in cells expressing only the α_{1C} subunit (only four out of eleven cells exhibited gating currents above the limits of detection, whereas eight out of eight β_{1A} coexpressing cells had measurable gating currents). The gating currents were integrated to measure the intramembrane charge movement (Q). The ON charge movement (Q_{on}) could be described by a Boltzmann distribution reaching a maximal value of $Q_{on,max}$.

4. The mean ratio of G_{max} : $Q_{on,max}$ increased from 99 ± 6 to 243 ± 30 pS fC^{-1} with β_{1A} coexpression, demonstrating that the β_{1A} subunit changes the gating of α_{1C} channels to favour the opening of the channels. However, this 2·5-fold change in the G_{max} : $Q_{on,max}$ ratio explains less than half of the 9·2-fold increase in G_{max} with β_{1A} subunit coexpression. The major effect is due to a 3·7-fold increase in $Q_{on,max}$, demonstrating that β_{1A} subunit coexpression increases the number of functional surface membrane channels.

Voltage-dependent Ca^{2+} channels are multi-subunit protein complexes in which the α_1 subunit forms the transmembrane pore. At least six different mammalian genes encode α_1 subunits, with the α_{1C} subunit being the isoform expressed in cardiac muscle (Zhang *et al.* 1993). Auxiliary subunits have been identified in a variety of tissues, including a cytoplasmic β subunit and a membrane-inserted α_2–δ subunit, as well as a γ subunit in skeletal muscle (Isom, De Jongh & Catterall, 1994). The β_{1A} subunit from skeletal muscle was the first to be identified (Ruth *et al.* 1989), and now four distinct β subunit genes with multiple splice variants are known (Isom *et al.* 1994).

Coexpression of the auxiliary subunits with the α_1 subunit can dramatically alter the properties of the expressed Ca^{2+} channels. Studies using *Xenopus laevis* oocytes to express the α_{1C} subunit demonstrated that coexpression of the β_{1A} subunit resulted in a large increase in ionic current as well as changes in the kinetics and voltage dependence of the current (Singer, Biel, Lotan, Flockerzi, Hofmann & Dascal, 1991; Neely, Wei, Olcese, Birnbaumer & Stefani, 1993). Expression in oocytes of a variety of α_1 and β isoforms have typically shown a significant increase in maximal current with β subunit coexpression (Mori *et al.* 1991; Williams *et al.* 1992). Experiments using mammalian cells to express the α_{1C} subunit have also demonstrated significant increases in peak current with β subunit coexpression, as well as changes in the kinetics of the currents (Pérez-García, Kamp & Marban, 1995, and references therein).

The mechanism of the increase in ionic current mediated by β subunit coexpression remains uncertain. There are several possible explanations: an increase in the number of functional channels; a greater probability of the channels being open; an increase in single-channel current; or a combination of these effects. Data from others argue against changes in single-channel current with β subunit coexpression (Wakamori, Mikala, Schwartz & Yatani, 1993). Equilibrium binding studies using radiolabelled dihydropyridines in transfected mammalian cells have shown an increase in the number of binding sites with

* To whom correspondence should be addressed.

This manuscript was accepted as a Short Paper for rapid publication.

β subunit coexpression without a change in affinity (Pérez-García *et al.* 1995). One interpretation of this finding is that β subunit coexpression results in an increase in the number of functional channels at the surface membrane. Alternatively, a study of gating currents using the cut-open oocyte technique concluded that there was no change in total intermembrane charge (Q_{max}) with β_{2A} coexpression, which suggested that there was no change in the number of functional channels (Neely *et al.* 1993). An increase in the ratio of maximal whole-cell conductance (G_{max}) to maximal charge movement (Q_{max}) was demonstrated, and so changes in coupling of the voltage sensor to channel gating were proposed to underlie the β_{2A}-induced increase in ionic current (Neely *et al.* 1993).

The goal of the present work was to examine charge movement associated with heterologously expressed Ca^{2+} channels in the mammalian HEK293 cell line, which we had previously used to demonstrate marked changes in dihydropyridine binding and current density with β_{1A} coexpression (Pérez-García *et al.* 1995). Initially, we established the utility of this mammalian heterologous expression system to study charge movement associated with the expressed Ca^{2+} channels. Secondly, the ionic currents and gating currents were examined in HEK293 cells transiently transfected with the α_{1C} subunit with or without β_{1A} ($\alpha_{1C} \pm \beta_{1A}$) subunit coexpression.

METHODS

HEK293 cell transfection

HEK293 cells (a human embryonic kidney cell line) were transiently transfected as previously described (Pérez-García *et al.* 1995). Briefly, the rabbit Ca^{2+} channel α_{1C} (Slish *et al.* 1989) and β_{1A} subunits (Pragnell, Sakamoto, Jay & Campbell, 1991) were subcloned into pGWIH, an expression vector with a cyto-megalovirus promoter (British Biotechnology Ltd, Oxford, UK). HEK293 cells were transiently transfected in 35 mm plates using the calcium phosphate precipitate method with 2–3 μg of DNA encoding the α_{1C} subunit $\pm$ β_{1A} subunits (1 : 1 molar ratio), SV40 T-antigen and β-galactosidase. Mock-transfected cells were transfected with 2 μg of DNA encoding β-galactosidase. Cells were studied 1–2 days after transfection.

Electrophysiology

Whole-cell patch clamp. The whole-cell configuration of the patch clamp technique (at 20–22 °C) was used to identify transfected HEK293 cells as previously described (Pérez-García *et al.* 1995). The composition of the internal solution was (mM): 120 CsCl, 5 MgATP, 10 EGTA and 10 Hepes (pH adjusted to 7·20 with CsOH). A dish of cells was mounted on the stage of an inverted microscope and perfused with (mM): 10 $BaCl_2$, 125 CsCl and 10 Hepes (pH 7·40 adjusted with CsOH). The bath solution was connected to ground via a 3 M KCl–agar bridge and a Ag–AgCl electrode. Whole-cell currents were recorded using a patch clamp amplifier (Axopatch 200, Axon Instruments, Inc.), sampled every 20–50 μs and filtered at 2–5 kHz (−3 dB, 4-pole Bessel filter). After establishing the whole-cell configuration, capacity transients were analogue-compensated, and series resistance was compensated by 60–80%. Currents were recorded following 25 ms test depolarizations repeated every 5 s to a family of potentials (−50 to +40 mV) from a holding potential of −60 or −80 mV. Data were leak-subtracted on-line using a $P/-4$ protocol from −60 mV preceding the test pulses. Where indicated, the data were fitted to a two-state Boltzmann distribution:

$$I = (V_m - V_{rev}) \times G_{max}/\{1 + \exp((V_{½} - V_m)/k)\},$$

where I is the measured peak current, V_m is the test membrane potential, V_{rev} is the extrapolated reversal potential, G_{max} is the maximal whole-cell conductance, $V_{½}$ is the mid-point potential and k is the slope factor.

Gating currents. Gating currents were measured after blocking ionic currents with the following solutions (mM): 0·1 $CdCl_2$, 10 $BaCl_2$, 125 CsCl and 10 Hepes (pH 7·40 with CsOH) or 2 $CdCl_2$, 0·1 $LaCl_3$, 8 $BaCl_2$, 125 CsCl and 10 Hepes (pH 7·40 with CsOH). Data were acquired as described above, with the exception that series resistance compensation was not used as it introduced high-frequency noise into the relatively small current signal. The linear leak and capacitative currents were subtracted digitally by scaling the mean of four leak pulses ($P/-4$) from −60 mV which preceded the test pulse. This leak subtraction protocol was chosen because it produced only linear capacitative currents and minimal linear leak currents. For cells with relatively small gating currents, i.e. most cells expressing only the α_{1C} subunit (α_{1C}-alone cells), two methods were employed to help resolve the gating currents. First, the linear capacitative current determined as above was fitted to a two- to three-exponential process before subtraction and secondly, multiple families (2–8 cycles) of identical depolarizing pulses were averaged. Changes in V_m approached completion in 200–300 μs after a change in command voltage, and data collected from this period were not displayed or analysed as indicated. Using the steady-state current as a baseline, the gating currents were then integrated to determine charge movement (Q). The relationship of charge movement (Q) as a function of V_m was fitted to a two-state Boltzmann distribution as follows:

$$Q = Q_{max}/\{1 + \exp((V_{½} - V_m)/k)\},$$

where Q_{max} is the maximal whole-cell charge movement, $V_{½}$ is the mid-point potential and k is the slope factor.

Statistics

Pooled data are expressed as the means $\pm$ S.E.M. Statistical comparisons were performed using Student's two-tailed t test, and values of $P < 0·05$ were considered statistically different. Both linear and non-linear regression analysis were employed to fit the data as indicated in the text.

RESULTS

Comparison of Ca^{2+} channel activation and charge movement

Transient transfection of HEK293 cells with cDNA encoding the $\alpha_{1C} \pm \beta_{1A}$ subunits of the Ca^{2+} channel has previously been demonstrated to result in the expression of functional L-type Ca^{2+} channels (Pérez-García *et al.* 1995). Figure 1*A* demonstrates inward currents elicited by 25 ms depolarizing test pulses from a holding potential of −60 mV using 10 mM Ba^{2+} as the charge carrier in a cell transfected with the $\alpha_{1C} + \beta_{1A}$ subunits. Closer inspection of the current records in Fig. 1*A* demonstrates a small initial outward current preceding the prominent inward current, suggesting the presence of detectable gating

currents associated with activation of the channels. In order to measure gating currents in this cell, the ionic current was blocked with 0·1 mM Cd^{2+} (Fig. 1*B*); however, a large inward tail current persisted. These ionic conditions were similar to those of Ertel, Smith, Leibowitz & Cohen (1994), who demonstrated that ON charge movement (Q_{on}) measured in the presence of 0·1 mM Cd^{2+} was quite similar to that measured in the presence of the Ca^{2+} channel toxin ω-agatoxin IIIA (ω-Aga IIIA) in intact guinea-pig atrial myocytes. The large inward tail currents have been described by others and suggested to be a combination of gating current and voltage-dependent relief of block of ionic current (Chow, 1991; Ertel *et al.* 1994). By increasing the external Cd^{2+} to 2 mM and adding 0·1 mM La^{3+} (Fig. 1*C*), all ionic current was blocked over a range of potentials up to 20 mV and Q_{on} (●) was equal to Q_{off} (○) (Fig. 2).

In order to confirm that the measured gating currents arise from the heterologously expressed Ca^{2+} channels, measurements were made in β-galactosidase-transfected HEK293 cells using the same ionic conditions (0·1 mM Cd^{2+}). Figure 1*D* shows a representative mock-transfected cell which underwent the same voltage protocol as the $\alpha_{1C} + \beta_{1A}$ transfected cell (Fig. 1*A–C*). No detectable gating currents were observed in this cell or in any of three other mock-transfected cells tested. This finding is consistent with our previous demonstration of the absence of endogenous I_{Ba} or I_{Ca} in these cells (Pérez-García *et al.* 1995), although endogenous Ca^{2+} currents have been reported by others in HEK293 cells (Berjukow, Doring & Hering, 1995). The presence of endogenous Ca^{2+} currents may be related to differences in the HEK293 cells propagated in different laboratories. Thus, this heterologous expression system allows the study of gating currents associated only with the expressed Ca^{2+} channels, obviating the need for subtraction protocols or depolarized holding potentials to discriminate gating from a variety of other channel types (Bean & Rios, 1989; Hadley & Lederer, 1991;

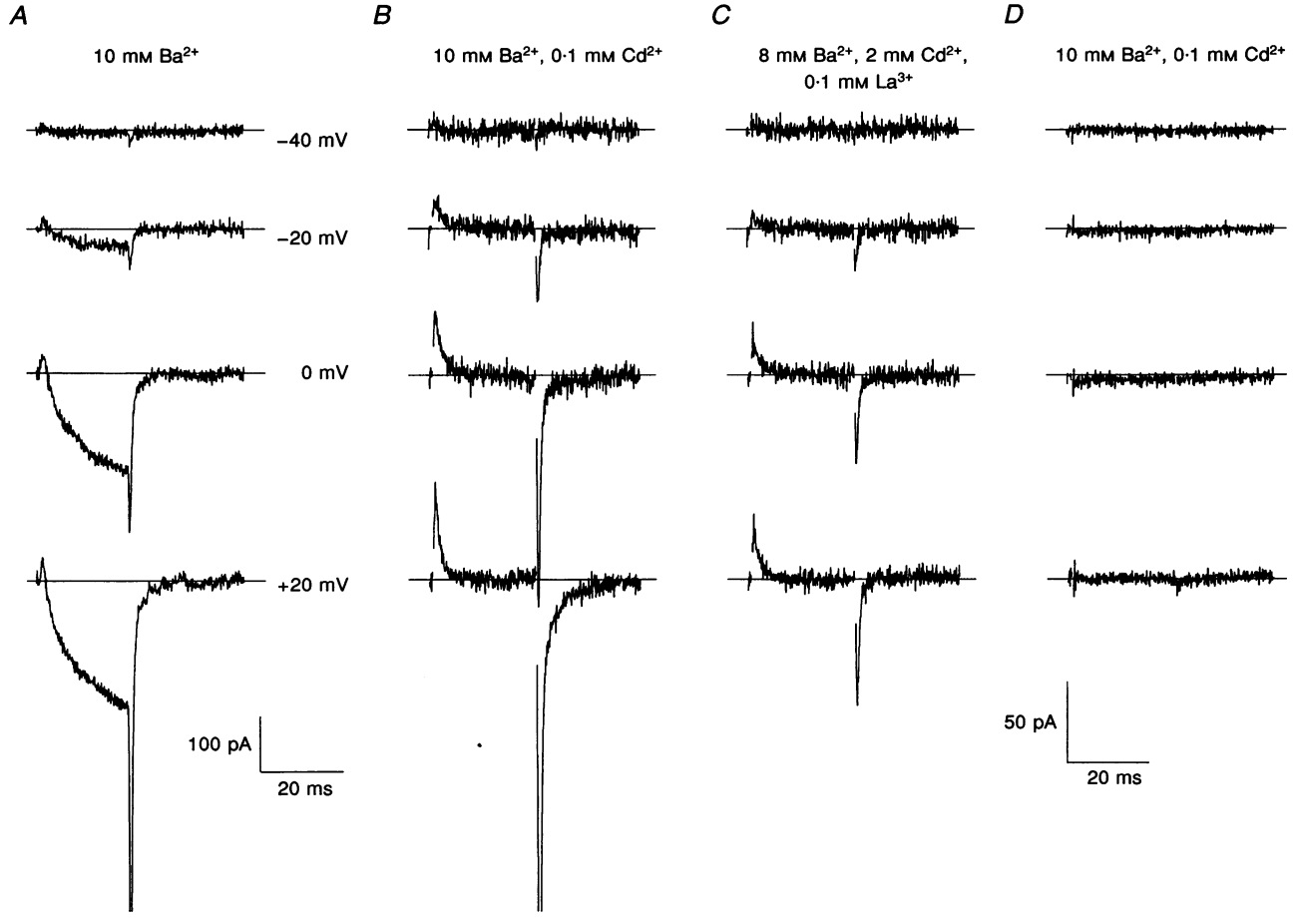

Figure 1. Ionic and gating currents in an HEK293 cell transfected with α_{1C} and β_{1A} subunits of the Ca^{2+} channel (*A–C*) compared with a control cell transfected with β-galactosidase (*D*)

A, ionic currents resulting from 25 ms depolarizations to the indicated test potentials carried by 10 mM Ba^{2+}. *B*, Cd^{2+} (0·1 mM) blocks ionic current during the test pulse isolating the ON gating current. *C*, Cd^{2+} (2 mM) and La^{3+} (0·1 mM) block ionic current, isolating both ON and OFF gating currents. *D*, current records using the same pulse protocol as in *A–C*, but in a control HEK293 cell transfected with β-galactosidase in 0·1 mM Cd^{2+}. Holding potential, −60 mV.

Ertel *et al.* 1994). In addition, the use of these relatively small cells allows for more rapid and uniform voltage control compared with adult cardiac myocytes with their extensive t-tubule system.

The voltage dependence of activation of the expressed Ca^{2+} channels was determined by plotting the whole-cell conductance (G) calculated from the peak ionic current (see Methods) as a function of V_m. For the same cell as shown in Fig. 1*A–C*, the relationship of G *vs.* V_m is shown in Fig. 2 (■) with the data fitted to a Boltzmann distribution ($G_{max} = 4{\cdot}3$ nS; $V_{½} = -2{\cdot}6$ mV; $k = 5{\cdot}9$ mV). To determine the non-linear charge movement associated with the activation of Ca^{2+} channels, the time integral of the ON gating currents (Q_{on}) in 0·1 mM Cd^{2+} was calculated and plotted as a function of V_m (Fig. 2, ▲). Non-linear charge movement can be fitted to a Boltzmann distribution (maximal Q_{on} value ($Q_{on,max}$) = 87 fC; $V_{½} = -20$ mV; $k = 5{\cdot}7$ mV), which demonstrates charge movement occurring over a more negative range of potentials than activation of whole-cell I_{Ba}. These data are consistent with the presence of voltage-dependent transition(s) which precede the opening of the channel.

Figure 2 also shows the calculated ON (●) and OFF (○) charge movement measured in 2 mM Cd^{2+}, 0·1 mM La^{3+} for this same cell. The Q_{on} data are well fitted by a Boltzmann distribution, but there are several remarkable differences from the data in 0·1 mM Cd^{2+}. Firstly, the voltage range over which charge movement occurs in 2 mM Cd^{2+}, 0·1 mM La^{3+} is shifted to the right ($V_{½} = -12$ mV) and the voltage dependence of charge movement is altered as k is 11 mV. Secondly, $Q_{on,max}$ (62 fC) was reduced by 28% compared with 0·1 mM Cd^{2+}. Similar differences were seen in four cells comparing non-linear charge movement in 0·1 mM Cd^{2+} with 2 mM Cd^{2+}, 0·1 mM La^{3+} from a holding potential of −80 mV ($\Delta Q_{on,max} = -25 \pm 10\%$; $\Delta V_{½} = 12 \pm 3{\cdot}6$ mV; $\Delta k = 7{\cdot}1 \pm 4{\cdot}0$ mV; not shown). These findings agree with published results using 2 mM Cd^{2+} in guinea-pig atrial cells, which demonstrated a decrease in the measured charge movement relative to that obtained using ω-Aga IIIA (Ertel *et al.* 1994). In addition, previous investigations have demonstrated that La^{3+} can have complex effects on the Na^+ channel gating process, which cannot be explained by simple surface charge effects (Armstrong & Cota, 1990). Therefore, all of the following data used 0·1 mM Cd^{2+} to isolate Q_{on} as a measure of charge movement in the transfected cells.

Effect of β_{1A} coexpression with α_{1C} on ionic and gating currents

Figure 3 shows current records in 10 mM Ba^{2+} resulting from a series of depolarizing command pulses for representative cells expressing the α_{1C} subunit alone (*A*) and the $\alpha_{1C} + \beta_{1A}$ subunits (*B*). A holding potential of −80 mV was chosen as currents were stable at this potential, whereas at −60 mV some cells exhibited a slow inactivation

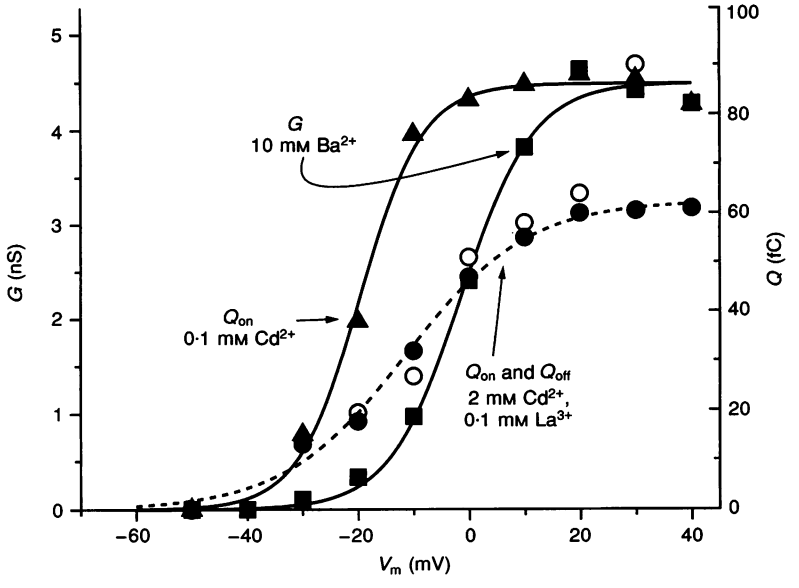

Figure 2. Voltage dependence of whole-cell conductance (G) and charge movement (Q) for the cell shown in Fig. 1*A–C*

G (■) calculated from the peak current was fitted by a Boltzmann distribution ($G_{max} = 4{\cdot}3$ nS; $V_{½} = -2{\cdot}6$ mV; $k = 5{\cdot}9$ mV). Q_{on} (▲) in 0·1 mM Cd^{2+} calculated from the time integral of the ON gating current could be fitted by a Boltzmann distribution ($Q_{on,max} = 87$ fC; $V_{½} = -20$ mV; $k = 5{\cdot}7$ mV). Q_{on} (●) and Q_{off} (○) calculated from the ON and OFF gating currents in 2 mM Cd^{2+} and 0·1 mM La^{3+} are plotted, and Q_{on} could be described by a Boltzmann distribution ($Q_{on,max} = 62$ fC; $V_{½} = -12$ mV; $k = 11$ mV). Holding potential, −60 mV. Whole-cell capacitance, 11 pF.

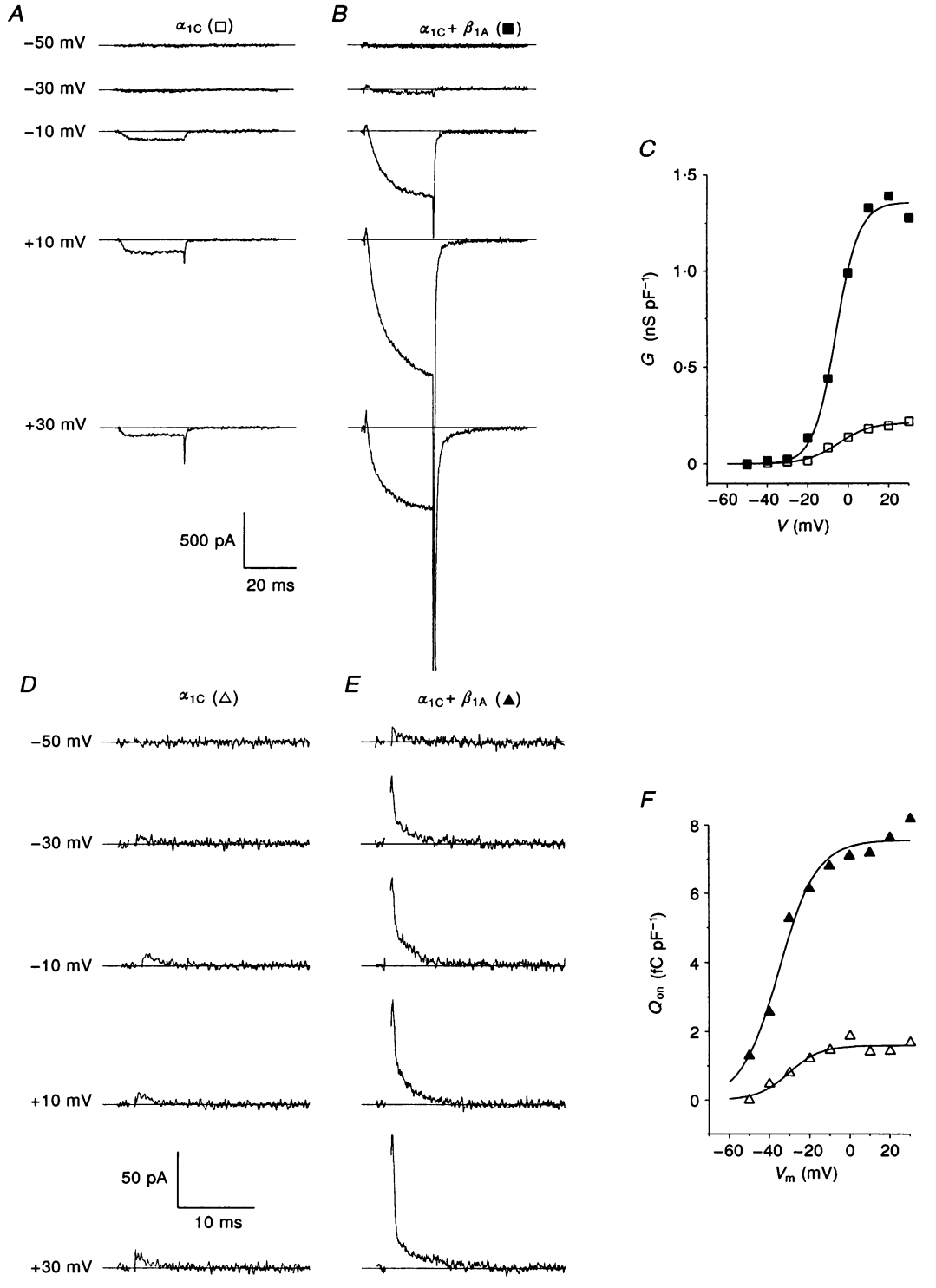

Figure 3. Comparison of ionic and gating currents of α_{1C} and $\alpha_{1C} + \beta_{1A}$ transfected cells

A and *B*, ionic currents (10 mM Ba^{2+}) are displayed at the indicated test potentials for representative cells expressing α_{1C} or $\alpha_{1C} + \beta_{1A}$ subunits. *C*, whole-cell conductance (G) is plotted as a function of membrane potential (V_m) for the α_{1C} (□) and $\alpha_{1C} + \beta_{1A}$ (■) expressing cells. Boltzmann distributions were fitted to the data and $G_{max} = 0{\cdot}16$ and $1{\cdot}35$ nS pF^{-1}, $V_{½} = -6{\cdot}8$ and $-6{\cdot}5$ mV and $k = 7{\cdot}6$ and $5{\cdot}7$ mV, respectively. *D* and *E*, ON gating currents in 0·1 mM Cd^{2+} for the same two cells expressing α_{1C} or $\alpha_{1C} + \beta_{1A}$ subunits. *F*, intramembrane charge movement determined from the gating currents displayed in *D* and *E* are plotted as a function of V_m for the α_{1C} (△) and $\alpha_{1C} + \beta_{1A}$ (▲) expressing cells. Boltzmann distributions were fitted to the data and $Q_{on,max} = 1{\cdot}6$ and $7{\cdot}3$ fC pF^{-1}, $V_{½} = -31$ and -33 mV and $k = 7{\cdot}8$ and $4{\cdot}0$ mV, respectively. Holding potential, −80 mV.

of I_{Ba}. As has been previously described, the ionic currents are larger with β_{1A} coexpression, and the brief 25 ms depolarizations clearly reveal the slowing of activation kinetics with β_{1A} coexpression (Pérez-García *et al.* 1995). The G–V relationships (Fig. 3*C*) demonstrate greater whole-cell conductance in the cell with the β_{1A} subunit co-expressed. The averaged data from a holding potential of −80 mV demonstrate a 9·2-fold increase in the normalized G_{max} with β_{1A} coexpression (91 ± 10 *vs.* 833 ± 107 pS pF^{-1}, $P < 0{\cdot}0001$) (Fig. 4*B*). The voltage dependence of channel activation occurs over a similar range of potentials, and average data comparing α_{1C}-alone ($n = 23$) with $\alpha_{1C} + \beta_{1A}$ ($n = 24$) cells showed mid-potentials for activation of −6·1 ± 1·1 and −6·6 ± 0·8 mV, respectively.

The same two cells were studied in the presence of 0·1 mM Cd^{2+} to enable a comparison of gating currents in the α_{1C} expressing cell (Fig. 3*D*) and $\alpha_{1C} + \beta_{1A}$ expressing cell (Fig. 3*E*). The gating currents and their time integrals (Q_{on}) (Fig. 3*F*) were markedly larger with β_{1A} subunit co-expression. The gating currents in the α_{1C}-alone cell were detectable but quite small. In seven out of eleven α_{1C} transfected cells with small but definite ionic currents measured in 10 mM Ba^{2+}, the gating currents were so small as to be below the resolution of the system (< 5 pA peak gating current) (Fig. 4*A*). In contrast, eight out of eight transfected cells with $\alpha_{1C} + \beta_{1A}$ subunits which were examined for both ionic and gating currents demonstrated easily resolvable gating currents. The voltage dependence

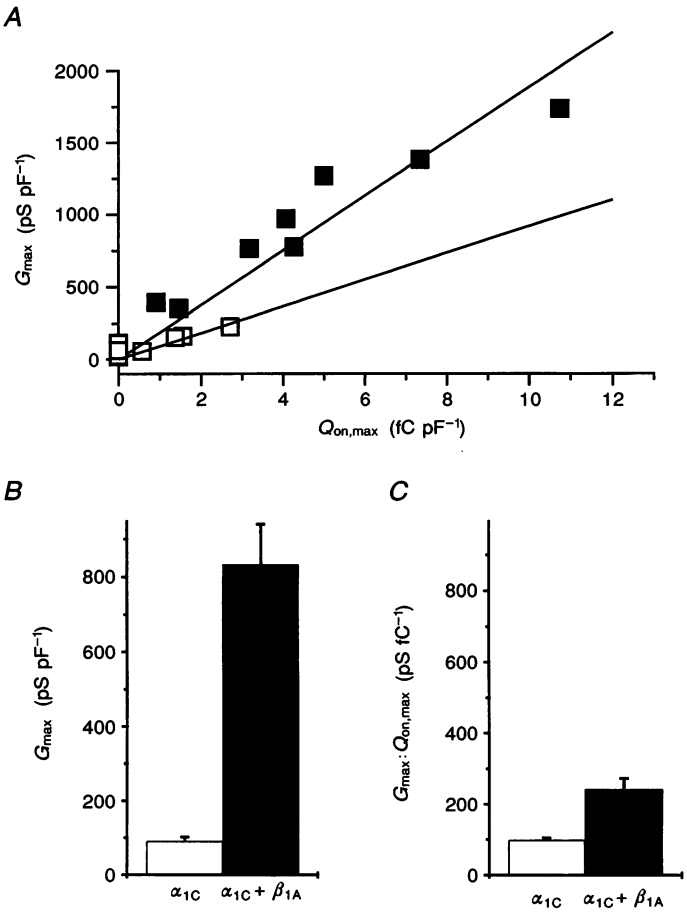

Figure 4. G_{max} and $Q_{on,max}$ comparison of α_{1C} *vs.* $\alpha_{1C} + \beta_{1A}$ transfected cells studied from a holding potential of −80 mV

A, for each cell studied, G_{max} and $Q_{on,max}$ are plotted comparing α_{1C} (□) with $\alpha_{1C} + \beta_{1A}$ (■) expressing cells. For seven out of eleven α_{1C}-alone cells with clear ionic currents, gating currents were below the limits of detection and are indicated by □ plotted on the ordinate. Linear regression analysis of the remaining four α_{1C} cells revealed a slope of 92 pS fC^{-1}. Linear regression of the $\alpha_{1C} + \beta_{1A}$ cells revealed a slope of 189 pS fC^{-1}. *B*, mean G_{max} determined from the Boltzmann fits of all twenty-three α_{1C} cells (□) compared with the mean G_{max} for all twenty-four $\alpha_{1C} + \beta_{1A}$ expressing cells (■). *C*, the mean ratio of G_{max} : $Q_{on,max}$ comparing four α_{1C} expressing cells (□) with eight $\alpha_{1C} + \beta_{1A}$ expressing cells (■). Error bars represent S.E.M.

of charge movement was similar comparing α_{1C} with $\alpha_{1C} + \beta_{1A}$ expressing cells ($V_{½} = -26{\cdot}5 \pm 2{\cdot}3$ and $-21{\cdot}1 \pm 2{\cdot}3$ mV; $n = 4$ and 8, respectively).

We next examined the relationship between the voltage sensors and channel opening by comparing the measured charge movement ($Q_{on,max}$) and whole-cell conductance (G_{max}) for each cell tested (Fig. 4*A*). If $Q_{on,max}$ is directly proportional to the number of channels expressed, then the relationship between G_{max} and $Q_{on,max}$ should be linear and pass through the origin. This predicted linear relationship has not been observed in native tissue, presumably due to the fact that ionic currents run down while charge movement does not (Bean & Rios, 1989; Hadley & Lederer, 1991). While I_{Ba} does occasionally run down in transfected HEK293, these cells were studied soon after access was obtained, and the HEK293 cells do not undergo any isolation procedure which, in native cells, could result in variable degrees of current run-down. The data for the $\alpha_{1C} + \beta_{1A}$ expressing cells (■) can be well fitted by a line through the origin (Fig. 4*A*). Most of the α_{1C}-alone cells (□) had gating currents below the resolution of this system, but for the four cells which did display measurable gating currents, a line through the origin provided a reasonable fit to the data. The mean ratios of $G_{max}:Q_{on,max}$ for α_{1C} expressing cells was 99 ± 6 compared with 243 ± 30 pS fC^{-1} ($P < 0{\cdot}01$) for $\alpha_{1C} + \beta_{1A}$ expressing cells (Fig. 4*C*). This increased ratio of $G_{max}:Q_{on,max}$ with β_{1A} subunit coexpression is consistent with the idea that the β subunit changes the coupling of the voltage sensor to channel opening, as observed using the *Xenopus* oocyte expression system (Neely *et al.* 1993). However, the 2·5-fold increase in the $G_{max}:Q_{on,max}$ ratio explains only a fraction of the overall 9·2-fold increase in G_{max}. The remaining difference in G_{max} must therefore be due to a 3·7-fold increase in $Q_{on,max}$ with β_{1A} subunit coexpression, which indicates a 3·7-fold increase in the number of functional channels.

In contrast, no change in $Q_{on,max}$ was observed in similar experiments using *Xenopus* oocytes to examine the effect of β_{2A} coexpression (Neely *et al.* 1993). This discrepancy could be explained by differences in the expression system used, i.e. mammalian cultured cells compared with amphibian oocytes. It is less likely to be due to differences in the β subunit coexpressed, as previous studies in oocytes have demonstrated similar increases in macroscopic current with the β_{1A} and β_{2A} subunits coexpressed with the α_{1C} subunit (Singer *et al.* 1991; Hullin *et al.* 1992). Furthermore, preliminary experiments using the β_{2A} subunit coexpressed in HEK293 cells have demonstrated similar results to β_{1A} coexpression (data not shown).

DISCUSSION

HEK293 cells have been used to express the $\alpha_{1C} \pm \beta_{1A}$ subunits of the L-type Ca^{2+} channel. Coexpression of the β_{1A} subunit was demonstrated to increase I_{Ba} due to a 9·2-fold increase in G_{max}. The mechanism of this increase in I_{Ba} can be attributed to both an increase in the probability of the channels being open (2·5-fold increase in $G_{max}:Q_{on,max}$) and to an increase in the number of functional channels (3·7-fold increase in $Q_{on,max}$). Possibly, the changes in gating can be ascribed to changes in the modes of gating of the channels. Single-channel studies will be needed to examine this issue. The putative increase in the number of functional channels may reflect changes in membrane trafficking by the β_{1A} subunit. Recent immunocytochemical studies using HEK293 cells have demonstrated that β_{2A} subunit coexpression results in increased surface membrane localization of the α_{1C} subunit without affecting the total amount of expressed α_{1C} subunit (Chien *et al.* 1995). The mechanism of the β subunit effect on the membrane trafficking of the α_{1C} subunit requires further investigation. A role for auxiliary subunits in modifying not only the gating, but also the membrane trafficking of channels, is emerging as a common theme as similar conclusions have been reached for Na^+ channels (Nuss, Chiamvimonvat, Pérez-García, Tomaselli & Marban, 1995).

Armstrong, C. M. & Cota, G. (1990). Modification of sodium channel gating by lanthanum. *Journal of General Physiology* **96**, 1129–1140.

Bean, B. P. & Rios, E. (1989). Nonlinear charge movement in mammalian cardiac ventricular cells. *Journal of General Physiology* **94**, 65–93.

Berjukow, S., Doring, F. & Hering, S. (1995). Endogenous calcium channels in human embryonic kidney (HEK) 293 cells. *Journal of Physiology* **487.P**, 209–210*P*.

Chien, A. J., Zhao, X., Shirokov, R. E., Puri, T. S., Chang, C. F., Sun, D., Rios, E. & Hosey, M. M. (1995). Roles of a membrane-localized β-subunit in the formation and targeting of functional L-type Ca^{2+} channels. *Journal of Biological Chemistry* **270**, 30036–30044.

Chow, R. H. (1991). Cadmium block of squid calcium currents. *Journal of General Physiology* **98**, 751–770.

Ertel, E. A., Smith, M. M., Leibowitz, M. D. & Cohen, C. J. (1994). Isolation of myocardial L-type calcium channel gating currents with spider toxin ω-Aga-IIIA. *Journal of General Physiology* **103**, 731–753.

Hadley, R. W. & Lederer, W. J. (1991). Properties of L-type calcium channel gating current in isolated guinea-pig ventricular myocytes. *Journal of General Physiology* **98**, 265–285.

Hullin, R., Singer-Lahat, D., Freichel, M., Biel, M., Dascal, N., Hofmann, F. & Flockerzi, V. (1992). Calcium channel β-subunit heterogeneity: functional expression of cloned cDNA from heart, aorta and brain. *EMBO Journal* **11**, 885–890.

Isom, L. L., De Jongh, K. H. & Catterall, W. A. (1994). Auxiliary subunits of voltage-gated ion channels. *Neuron* **12**, 1183–1194.

Mori, Y., Friedrich, T., Kim, M.-S., Mikami, A., Nakai, J., Ruth, P., Bosse, E., Hofmann, F., Flockerzi, V., Furuichi, T., Mikoshiba, K., Imoto, K., Tanabe, T. & Numa, S. (1991). Primary structure and functional expression from complementary DNA of a brain calcium channel. *Nature* **350**, 398–402.

Neely, A., Wei, X., Olcese, R., Birnbaumer, L. & Stefani, E. (1993). Potentiation by the beta subunit of the ratio of the ionic current to the charge movement in the cardiac calcium channel. *Science* **262**, 575–578.

Nuss, H. B., Chiamvimonvat, N., Pérez-García, M. T., Tomaselli, G. F. & Marban, E. (1995). Functional association of β_1 subunit with human cardiac (hH1) and rat skeletal muscle (μ1) sodium channel α subunits expressed in *Xenopus* oocytes. *Journal of General Physiology* **106**, 1171–1191.

Pérez-García, M. T., Kamp, T. J. & Marban, E. (1995). Functional properties of cardiac L-type calcium channels transiently expressed in HEK293 cells. *Journal of General Physiology* **105**, 289–306.

Pragnell, M., Sakamoto, J., Jay, D. & Campbell, K. P. (1991). Cloning and tissue-specific expression of the brain calcium channel β-subunit. *FEBS Letters* **291**, 253–258.

Ruth, P., Rohrkasten, A., Biel, M., Bosse, E., Regulla, S., Meyer, H. E., Flockerzi, V. & Hofmann, F. (1989). Primary structure of the β-subunit of the DHP-sensitive calcium channel from skeletal muscle. *Science* **245**, 1115–1118.

Singer, D., Biel, M., Lotan, I., Flockerzi, V., Hofmann, F. & Dascal, N. (1991). The roles of the subunits in the function of the calcium channel. *Science* **253**, 1553–1557.

Slish, D. F., Engle, D. B., Varady, G., Lotan, I., Singer, D., Dascal, N. & Schwartz, A. (1989). Evidence for the existence of a cardiac specific isoform of the α_1 subunit of the voltage-dependent calcium channel. *FEBS Letters* **250**, 509–514.

Wakamori, M., Mikala, G., Schwartz, A. & Yatani, A. (1993). Single-channel analysis of a cloned human heart L-type Ca^{2+} channel alpha 1 subunit and effects of a cardiac beta subunit. *Biochemical and Biophysical Research Communications* **196**, 1170–1176.

Williams, M. E., Feldman, D. H., McCue, A. F., Brenner, R., Velicelebi, G., Ellis, S. B. & Harpold, M. M. (1992). Structure and functional expression of α_1, α_2, and β subunits of a novel human neuronal calcium channel subtype. *Neuron* **8**, 71–84.

Zhang, J., Randall, A. D., Ellinor, P. T., Horne, W. A., Sather, W. A., Tanabe, T., Schwarz, T. L. & Tsien, R. W. (1993). Distinctive pharmacology and kinetics of cloned neuronal Ca^{2+} channels and their possible counterparts in mammalian CNS neurons. *Neuropharmacology* **32**, 1075–1088.

Acknowledgements

The authors wish to thank Maria Janecki for technical support. This work was supported by grants from the NIH (R01 HL 36597 to E.M.), Howard Hughes Medical Institute (post-doctoral fellowship for physicians to T.J.K.) and Fundacion Ramon Areces (fellowship to M.T.P.-G.)

Received 4 December 1995; accepted 10 February 1996.